Original Article

YC-1 exerts inhibitory effects on MDA-MB-468 breast cancer cells by targeting EGFR *in vitro* and *in vivo* under normoxic condition

Ying Cheng[1], Wei Li[2], Ying Liu[1], Huan-Chen Cheng[2], Jun Ma[2] and Lin Qiu[2]

Abstract

3-(5′-hydroxymethyl-2′-furyl)-1-benzyl indazole (YC-1), the hypoxia-inducible factor-1 alpha (HIF-1α) inhibitor, suppresses tumor proliferation and metastasis by down-regulating HIF-1α expression under hypoxic conditions. Our previous studies demonstrated that YC-1 inhibited breast cancer cell proliferation under normoxic conditions. In the current study, we investigated the targets of YC-1 and mechanism of its action in MDA-MB-468 breast cancer cells. In the *in vitro* experiments, we found that YC-1 significantly inhibited MDA-MB-468 cell proliferation in normoxia and hypoxia. Under normoxic conditions, YC-1 induced apoptosis of MDA-MB-468 cells and blocked cell cycle in the G$_1$ phase, and these effects were possibly related to caspase 8, p21, and p27 expression. RT-PCR and Western blotting results showed that YC-1 primarily inhibited HIF-1α at the mRNA and protein levels under hypoxic conditions, but suppressed the expression of epidermal growth factor receptor (EGFR) at the mRNA and protein levels under normoxic conditions. *In vivo*, YC-1 prolonged survival, increased survival rate, decreased tumor size and metastasis rate, and inhibited tissue EGFR and HIF-1α expression. However, YC-1 exerted no obvious effect on body weight. These results indicate that YC-1 inhibits the proliferation of MDA-MB-468 cells by acting on multiple targets with minimal side effects. Thus, YC-1 is a promising target drug for breast cancer.

Key words Breast cancer, YC-1, normoxic condition, EGFR, HIF-1α, MDA-MB-468 cell

3-(5'-hydroxymethyl-2'-furyl)-1-benzyl indazole (YC-1) was initially reported as a novel activator of soluble guanylyl cyclase with a pharmacologic mechanism that included anti-platelet aggregation and vascular relaxation[1,2]. More recent studies revealed that YC-1 can also inhibit angiogenesis and suppress tumors[3]. YC-1 suppresses cell proliferation in liver cancer, pancreatic cancer, prostate cancer, lung cancer, breast cancer, leukemia, and other cancers [4-7] and has a relatively broad spectrum of antitumor activities. YC-1 was reported to induce cell apoptosis and block cell cycle progression under hypoxic conditions by inhibiting the expression of hypoxia-inducible factor-1 alpha (HIF-1α).

Under normoxic conditions, the antitumor effect of YC-1 is related with nuclear factor-kappa B (NF-κB) [8], the c-Jun N-terminal kinase (JNK) signaling pathway [9], and cyclic GMP (cGMP) [10]. Our previous studies revealed that YC-1 suppressed the proliferation of MDA-MB-468 breast cancer cells by inhibiting HIF-1α expression under both hypoxia and normoxia[10]. In this study, we analyzed the inhibitory effect of YC-1 on MDA-MB-468 breast cancer cells under normoxic conditions to determine its underlying mechanism.

Materials and Methods

Major drugs and agents

YC-1 was purchased from Sigma, dissolved in DMSO to a concentration of 10 mol/L, and stored at −20℃ for subsequent analysis. Cobalt (II) chloride (CoCl$_2$) solution was purchased from Sigma. Lysis buffer was purchased from HaiGene Co., Ltd. Epidermal

Authors' Affiliations: [1]Jilin Tumor Hospital, Changchun, Jilin 130012, P. R. China; [2]Harbin Institute of Hematology and Tumor, Harbin, Heilongjiang 150010, P. R. China.

Corresponding Author: Lin Qiu, Harbin Institute of Hematology and Tumor, Harbin, Heilongjiang 150010, P. R. China. Tel: +86-451-84883432; Email: qiulin@csco.org.cn.

growth factor receptor (EGFR) and HIF-1α antibodies were supplied by UpSTATe. P21 and P27 antibodies were purchased from Santa Cruz. Caspase 3, Caspase 8, and Caspase 9 antibodies were bought from BioVision. STAT3 and phospho-STAT3 antibodies were supplied by Cell Signaling. β-actin and β-tubulin antibodies were purchased from Huate Biotechnology, Inc. Propidium iodide (PI) was purchased from Sigma and Annexin V-FITC was purchased from BD company. RNAiso Plus was purchased from TaKaRa. TaqMan Reverse Transcription Reagents was purchased from ABI company. SYBR Green qPCR Supermix was purchased from TransGen Biotech, Inc. Primer synthesis was performed by Sangon Biotech (Shanghai) Co., Ltd. Immunohistochemical kits and the EGFR and HIF-1α monoclonal antibodies were bought from Boster BioTech Co., Ltd. pGL3 luciferase reporter vector and D-luciferin were supplied by Promega. Lipofectamine™ 2000 was purchased from Invitrogen.

Cell culture and treatment

MDA-MB-468 breast cancer cells were kindly provided by Professor Amin from MD Anderson Cancer Center (Houston, TX, USA). Cells were passaged in DMEM medium containing 10% fetal calf serum. $CoCl_2$ (100 μmol/L) was used to stimulate hypoxic conditions.

MTT analysis

MDA-MB-468 cells were seeded in triplicate into 96-well plates at a density of 2×10^4/well. Cells were allowed to attach for 24 h and then were supplemented with 1, 3, 10 μmol/L of YC-1, respectively, with or without 100 μmol/L of $CoCl_2$, and incubated for another 24 h. After adding 20 μL of MTT (5 mg/mL) in each well, the cells were incubated for 4 h. The supernatant was discarded from each well and replaced with 180 μL of DMSO. The absorbance value at 490 nm (A_{490}) of each well was detected three times by using a microplate reader. The proliferation rate was calculated by the formula: proliferation rate = (A_{490} in the experimental group / A_{490} in the control group) × 100%.

Flow cytometry for apoptosis and cell cycle detection

Approximately 2×10^6 MDA-MB-468 cells were placed in a culture dish and allowed to attach for 24 h, after which they were supplemented with various concentrations of YC-1, with or without $CoCl_2$, and cultured for 24 h in normoxic condition. Cells were then digested with 0.25% trypsin and collected, rinsed twice with pre-cooled PBS, and prepared for apoptosis and cell cycle analysis.

For apoptosis analysis, cells were adjusted to a density of 1×10^6/mL with binding buffer. Annexin V-FITC and 50 μg/mL PI were added to the cell solution. The mixture was gently shaken, kept in the dark for 15 min at room temperature, and subjected to flow cytometry analysis. All samples were assayed in triplicate.

For cell cycle analysis, 2 mL of pre-cooled 70% ethanol was added, and the cells were fixed overnight at 4℃. Next, the cells were rinsed twice with pre-cooled PBS, supplemented with 400 μL of PI (50 μg/mL), kept in the dark for 30 min at room temperature, and then subjected to flow cytometry analysis. All samples were assayed in triplicate.

Western blotting

Approximately 2×10^6 MDA-MB-468 cells were placed in a culture dish and allowed to attach for 24 h. Various concentrations of YC-1 were then added, respectively, with or without $CoCl_2$, and the cells were cultured for 8 h before being digested. The protein was extracted with lysis buffer and concentration was measured using a microplate reader. A portion of 40 μg protein sample was collected from each group, boiled for 10 min, loaded onto 10% SDS-PAGE gels, and then transferred to PVDF membranes with electroblotting. Membranes were blocked for 1 h with 5% fat-free milk at room temperature, rinsed with PBS, and incubated with diluted primary antibodies (EGFR, HIF-1α, P21, P27, STAT3, phospho-STAT3, β-actin, and β-tubulin at 1:1000 dilution; Caspase 3, Caspase 8, and Caspase 9 at 1:400 dilution) overnight at 4℃. Then, membranes were incubated with specific secondary antibodies (1:1000) for 2 h and rinsed with PBS. Proteins were detected by using chemilumi-nescence.

Fluorescent quantification polymerase chain reaction (FQ-PCR) analysis

Approximately 2×10^6 MDA-MB-468 cells were placed in culture dish and allowed to attach for 24 h. Various concentrations of YC-1 were added into culture dish, respectively, and the cells were cultured for 8 h in normoxic or hypoxic condition. Total RNA was extracted by using RNAiso Plus reagent (TaKaRa Company, Japan) according to the manufacturer's protocol. One μg of RNA was used for reverse transcription reaction with TaqMan Reverse Transcription Reagents. The reaction mixture contained 1.0 μL of 10× RT Buffer, 2.0 μL of dNTP (10 mmol/L), 2.2 μL of $MgCl_2$ (25 mmol/L), 0.2 μL of RNase inhibitor (20 U/μL), 0.5 μL of Random Hexamer (50 μmol/L), 0.625 μL of Multiscribe Reverse Transcripase (50 U/μL), and dH_2O with a final volume of 10 μL. The reaction conditions were as follows: 25℃ for 10 min, 37℃ for 60 min, and then 95℃ for 5 min.

FQ-PCR system contained 1.0 μL of each reverse

primer, 25 μL of 2× qPCR supermix, 1.0 μL of passive preference dye, 1.0 μL of cDNA, and dH$_2$O with a final volume of 50 μL. The FQ-PCR reaction conditions were as follows: 95℃ for 5 min; 45 cycles of 95℃ for 15 s, 55℃ for 15 s, 72℃ for 45 s. Relative quantitative analysis was performed three times using the Δ Δ Ct method. Primers for this experiment are given below.

EGFR forward primer, 5′-GACAGCTATGAGATGGA GGAA-3′; reverse primer, 5′-GAGTCACCCCTAAATGC CA-3′; amplification fragment length 198 bp.

HIF-1α forward primer, 5′-CGTGTTATCTGTCGCT TTGAGTC-3′; reverse primer, 5′-GTCTGGCTGCTGT AATAATGTTCC-3′; amplification fragment length 140 bp.

GAPDH forward primer, 5′-GGATTTGGTCGTATTG GG-3′; reverse primer, 5′-GGAAGATGGTGATGGGA TT-3′; amplification fragment length 205 bp.

Establishment of tumor-bearing mouse models

Female BALB/c nude mice, weighing 18−20 g, were supplied by Heilongjiang University of Chinese Medicine (certificate number: 09-3-3). Approximately 1 × 10^6 MDA-MB-468 cells in log phase were inoculated in nude mice via armpit injection under sterile conditions. One week later, these mice were randomly divided into the control group (n = 8), low-dose group (n = 10), and high-dose group (n = 10) and underwent daily intraperitoneal injection of 10% DMSO, 30 mg/kg YC-1, or 100 mg/kg YC-1, respectively, for 13 weeks. The mice were euthanized on the second day after the final injection and tumor tissues were collected. A portion of the tumor samples were used for total RNA extraction and reverse transcription. The remaining samples were fixed in 10% formaldehyde and then paraffin-embedded for histological section.

Immunohistochemical detection of tissue EGFR and HIF-1α expression

The procedure was performed strictly according to the manufacturer's protocol (Boster BioTech Co., Ltd.). Positive cells were defined as those with a colorless background and brownish yellow-stained cytoplasm and/or nucleus.

Measurement of tumor volume *in vivo*

MDA-MB-468 cells were transfected with pGL3 luciferase reporter plasmid by using Lipofectamine 2000 according to the manufacturer's instructions. At 24 h after transfection, cells were selected with culture solution containing G418 (500 μg/mL) for 3 weeks to establish cell lines stably expressing luciferase. Approximately 1 × 10^6 stably transfected cells in log phase were inoculated into nude mice via the armpit in sterile conditions. The mice were divided into the DMSO group (n = 3) and the YC-1 group (100 mg/kg, n = 3). Tumor volume was measured using *in vivo* imaging system (IVIS200, Xenogen Inc., USA) on day 0, 14, and 28. Prior to imaging, 0.2 mL D-luciferin (15 mg/mL) was administered via the tail vein and the mice were anesthetized with isoflurane.

Statistical analysis

SPSS 13.0 software was used for statistical analysis. The data are presented as mean ± standard deviation. Mean values between two groups were compared by using t-test. Mean values among multiple groups were statistically analyzed by using chi-square test. A value of P < 0.05 was considered significant.

Results

Effect of YC-1 on cell proliferation

MTT results showed that after 24 h of YC-1 treatment at different concentrations (1, 3, and 10 μmol/L), the proliferation of MDA-MB- 468 cells was significantly inhibited in a dose-dependent manner under both normoxia and hypoxia (P < 0.001, Figure 1). Our previous study showed that a large proportion of MDA-MB-468 cells died 48 h and 72 h after low-dose YC-1 under normoxic conditions, and no significant difference was noted after treatment of 1, 3, and 10 μmol/L YC-1 (data not published). Hence, the treatment time was designed as 24 h.

Effect of YC-1 on HIF-1α expression

We next measured the effect of YC-1 on the expression of HIF-1α. MDA-MB-468 cells treated with YC-1 under normoxic and hypoxic conditions were analyzed for expression of HIF-1α at mRNA and protein levels by using RT-PCR and Western blotting, respectively. As shown in Figures 2A and 2B, YC-1 significantly inhibited the HIF-1α mRNA expression in MDA-MB-468 cells under normoxia at a dose of 10 μmol/L (P < 0.05), whereas it had no effect on the expression of HIF-1α at the protein level. However, YC-1 inhibited HIF-1α expression at the mRNA and protein levels in a dose-dependent manner under hypoxic conditions (Figures 2C and 2D). Collectively, these results indicate that HIF-1α is not the target of the inhibitory effect of YC-1 in MDA-MB-468 cells under normoxic conditions.
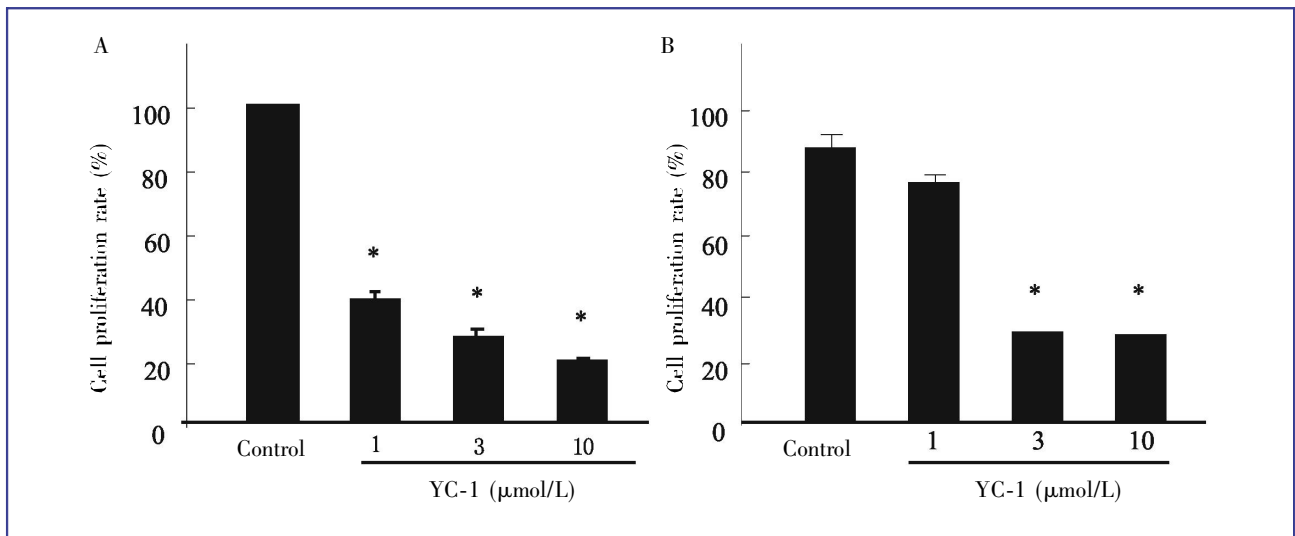
Figure 1. Effect of YC-1 on MDA-MB-468 cell proliferation under normoxia and hypoxia. A, YC-1 inhibits MDA-MB-468 cell proliferation significantly under normoxia. B, YC-1 (3 and 10 μmol/L) inhibits MDA-MB-468 cell proliferation significantly under hypoxia. *$P < 0.001$, vs. control.
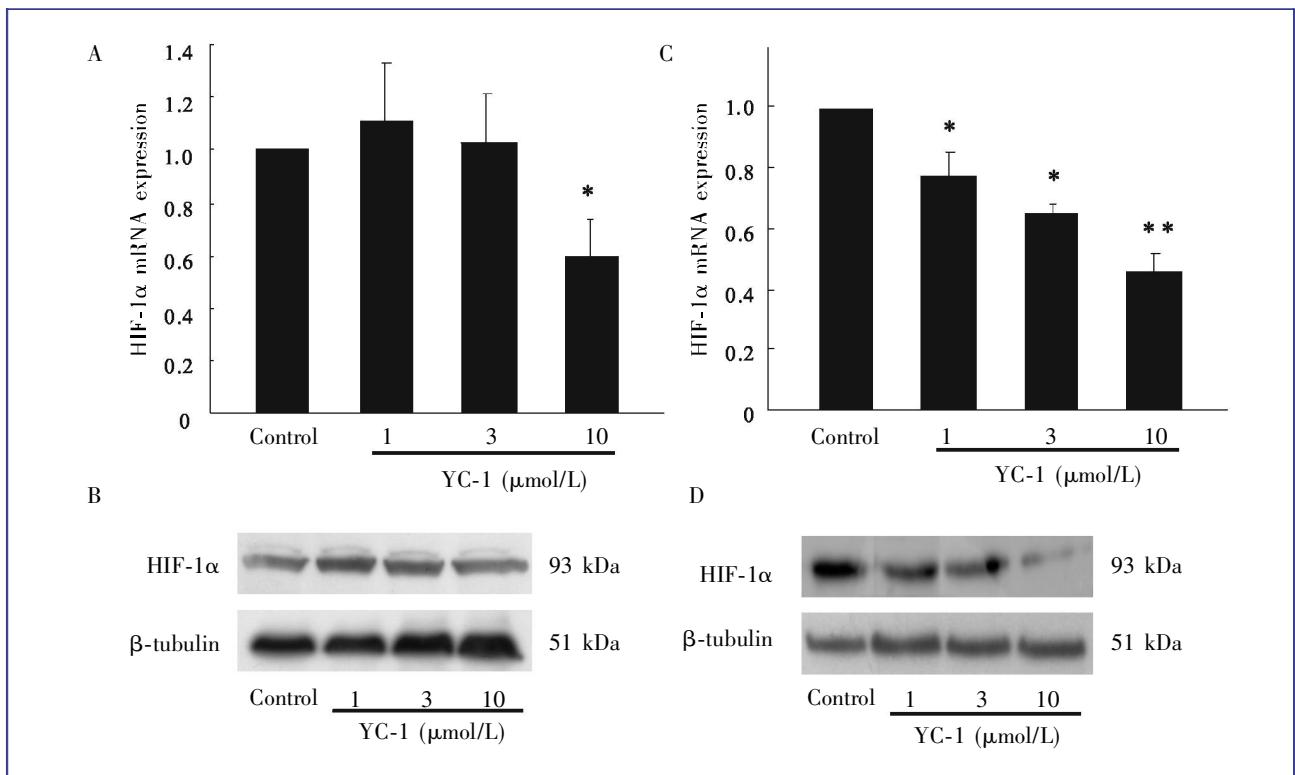
Figure 2. Effect of YC-1 on the HIF-1α expression in MDA-MB-468 cells. Under normoxic conditions, 10 μmol/L YC-1 inhibited *HIF-1α* mRNA expression(A), but had no effect on HIF-1α protein(B). Under hypoxic conditions, YC-1 inhibited HIF-1α mRNA(C) and protein expression (D) in a dose-dependent manner. *$P < 0.05$, **$P < 0.01$, vs. control.

Effect of YC-1 on EGFR and STAT3 expression

Because MDA-MB-468 cells highly express EGFR, we hypothesized that EGFR is related with the underlying mechanism of the inhibitory effects of YC-1 in MDA-MB-468 cells under normoxia. The effect of YC-1

on EGFR and STAT3 expression in MDA-MB-468 cells was analyzed by using RT-PCR and Western blotting. In a normoxic environment, low-dose YC-1 (1 μmol/L) inhibited the expression of EGFR at both mRNA and protein levels in a dose-dependent manner (Figures 3A and 3B). In addition, YC-1 (1 μmol/L) also inhibited the expression of downstream signaling pathway components STAT3 and phospho-STAT3. However, only high-dose YC-1 (10 μmol/L) inhibited the expression of EGFR at mRNA and protein levels in cells exposed to a hypoxic environment (Figures 3C and 3D). Thus, YC-1 induced inhibition of MDA-MB-468 cell proliferation was associated with the expression of EGFR protein.

Effect of YC-1 on cell apoptosis and cell cycle

The EGFR signaling pathway regulates apoptosis, cell cycle progression, proliferation, differentiation, and migration of tumor cells. Therefore, we used flow cytometry and Western blotting to detect the influence of
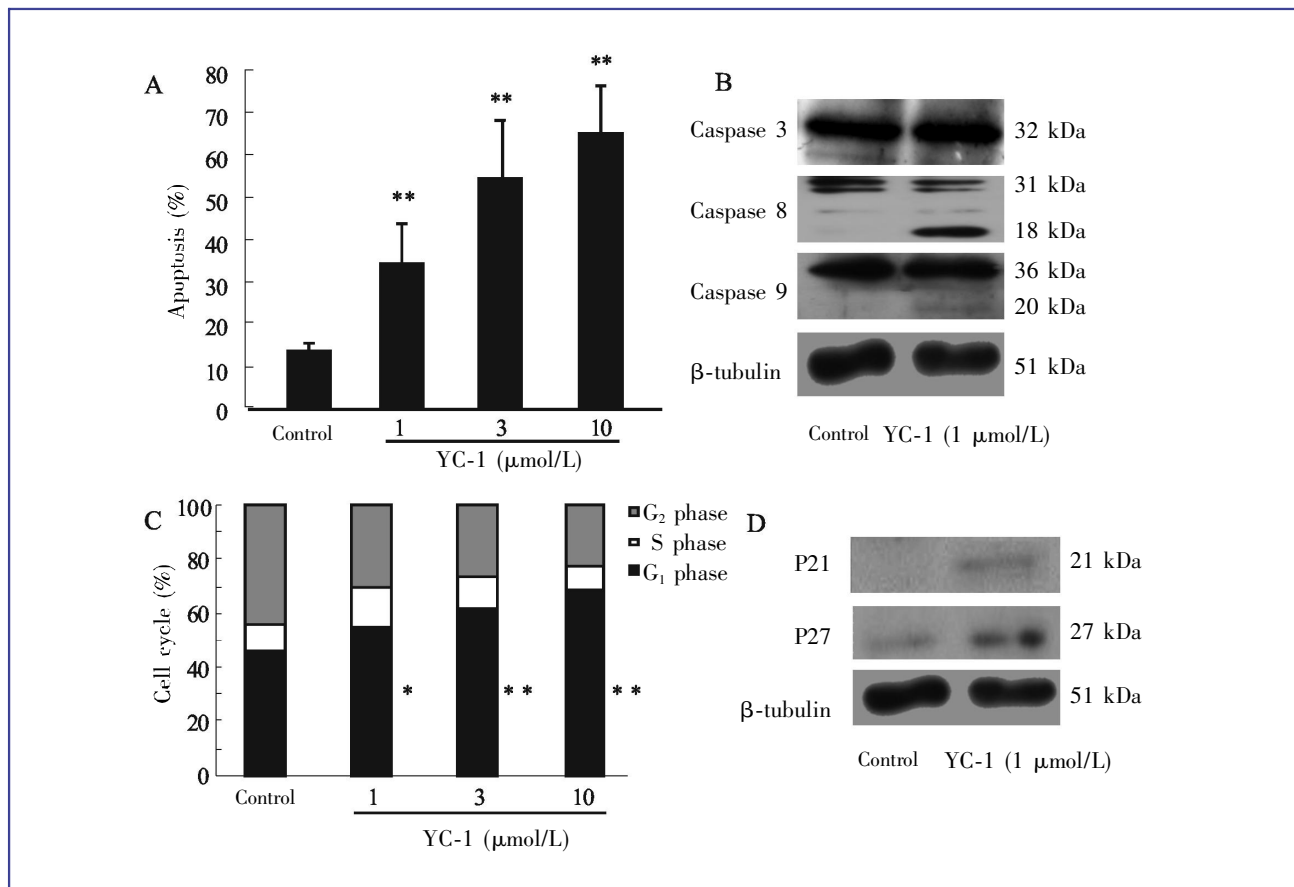
YC-1 on apoptosis and cell cycle progression of MDA-MB-468 cells under normoxia. As shown in Figures 4A and 4B, YC-1 at various concentrations (1, 3, and 10 μmol/L) significantly promoted apoptosis of MDA-MB-468 cells ($P < 0.01$), and these effects were likely associated with the Caspase 8 pathway but not with the Caspase 9 or Caspase 3 pathway. YC-1 at different concentrations arrested the cell cycle in G_1 phase ($P < 0.05$, Figure 4C), and these effects were probably due to increased expression of P21 and P27 (Figure 4D).

Effect of YC-1 on nude mouse models

To investigate whether *in vitro* and *in vivo* mechanisms of YC-1 action are identical, we established nude mouse models by injecting BALB/c mice with MDA-MB-468 cells. Thirteen weeks after intraperitoneal injection of YC-1, the results showed that YC-1 at doses of 30 and 100 mg/kg significantly inhibited the proliferation of breast cancer cells compared to the control group.
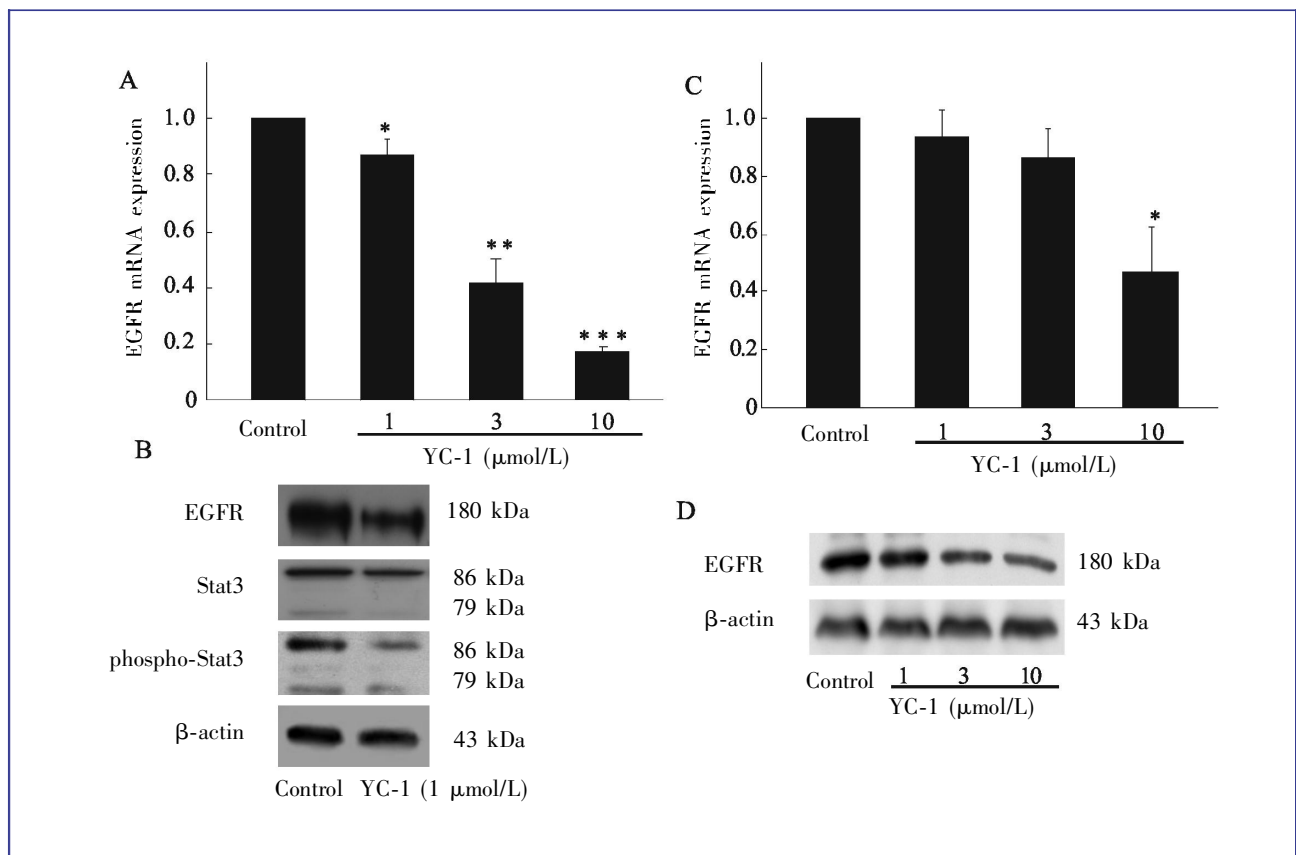
Figure 3. Effect of YC-1 on EGFR and STAT3 expression in MDA-MB-468 cells. Under normoxic conditions, YC-1 inhibited EGFR mRNA expression in a dose-dependent manner (A); YC-1 (1 μmol/L) also inhibited the expression of EGFR and STAT3 and blocked STAT3 phosphorylation (B). Under hypoxic conditions, only 10 μmol/L YC-1 inhibited EGFR mRNA (C) and protein expression (D). *$P < 0.05$, **$P < 0.01$, ***$P < 0.001$, vs. control.

Figure 4. Effects of YC-1 on apoptosis and cell cycle progression of MDA-MB-468 cells. A, YC-1 promoted apoptosis in a dose-dependent manner. B, the expression of Caspase 8 increased, but the expression of Caspase 3 and Caspase 9 were not obviously changed after YC-1 treatment. C, YC-1 induced cell cycle arrest at G_1 phase. D, the expression of P21 and P27 increased after YC-1 treatment. *$P < 0.05$, **$P < 0.01$, vs. control.

Notably, there was no obvious increase in tumor size in the 100 mg/kg group (Figures 5A and 5B). By 24 weeks after treatment, all mice in the control group died. By 40 weeks, approximately 40% of mice were alive in the 30 mg/kg group and 90% were alive in the 100 mg/kg group (Figure 5C). In the control group, all mice had tumor metastasis after 19 weeks, whereas no metastasis was noted in the YC-1 treatment groups. Thirty-six weeks after treatment, 70% of mice in the low-dose group had tumor metastasis compared to only 10% in the high-dose group (Figure 5D). No statistical significance was noted in the weight of nude mice among the control and YC-1 treatment groups (Figure 5E). Furthermore, compared with the mice in the control group, the mice in the YC-1 treatment groups had no significant differences in movement activity or fur color. Immunohistochemical analysis indicated that YC-1 at doses of 30 mg/kg and 100 mg/kg significantly inhibited the expression of EGFR and HIF-1α in tumor-bearing nude mice compared to

those in the control group (Figure 5F).

Discussion

Because MDA-MB-468 cells highly express EGFR, we hypothesized that the inhibitory effect of YC-1 on these cells is associated with EGFR. Our studies confirmed that YC-1 inhibited the proliferation of MDA-MB-468 cells under normoxia and hypoxia by acting on different targets. Under hypoxic conditions, YC-1 mainly targets the expression of HIF-1α , but under normoxic conditions, YC-1 inhibits EGFR expression. To date, no studies focusing on the inhibitory effect of YC-1 on EGFR have been reported. Hence, in current study, we explored a novel target of YC-1.

The positive rate of EGFR expression is high in breast cancer patients, ranging from 14% to 65%[11]. The EGFR signaling pathway has been found to regulate
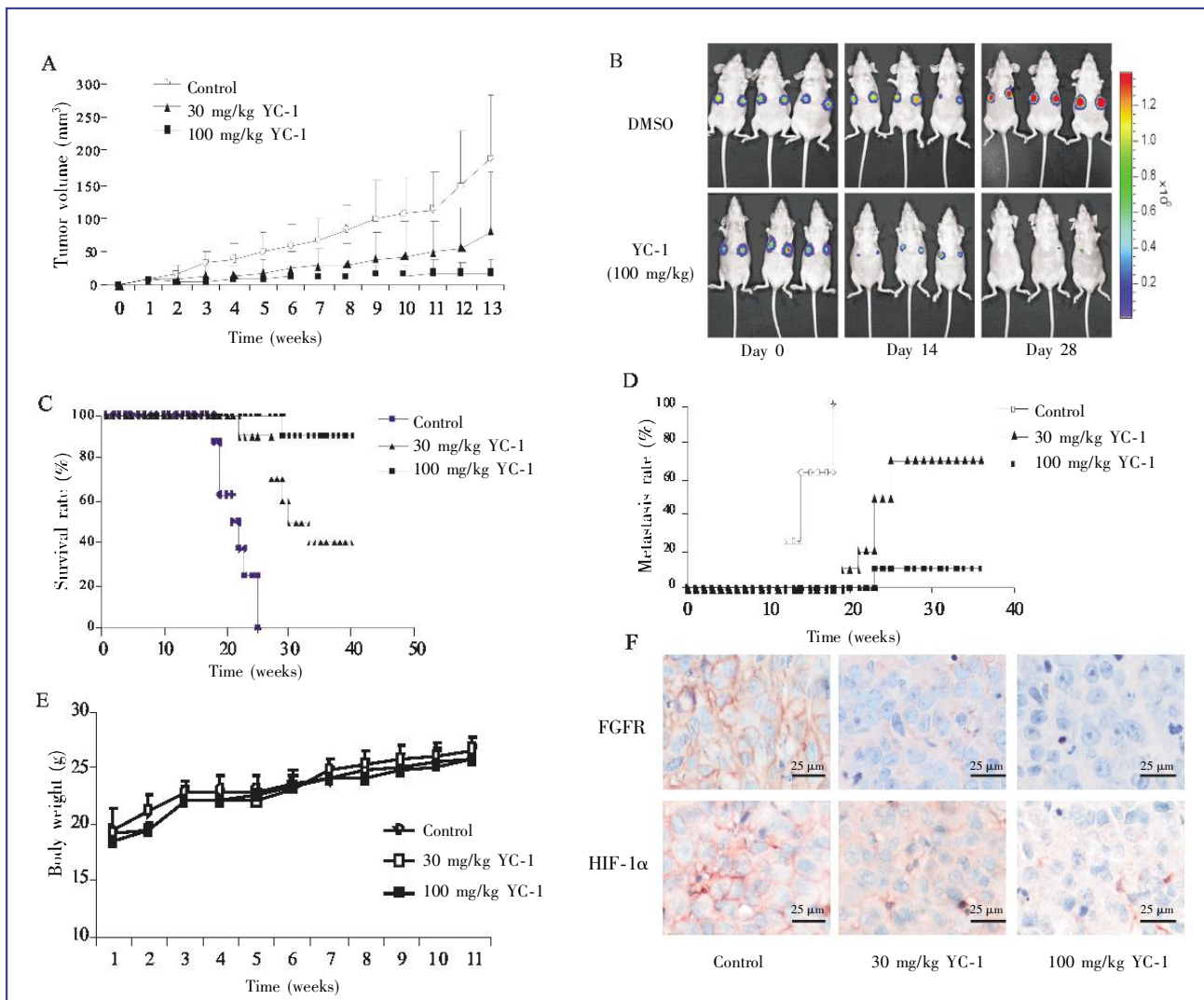
Figure 5. Effect of YC-1 on the mouse xenograft model. A, compared with control, 30 and 100 mg/kg of YC-1 significantly inhibited tumor growth. Notably, tumor volume in the 100 mg/kg YC-1 group was not augmented. B, *in vivo* optical imaging revealed that the tumor volume in the 100 mg/kg YC-1 group decreased over time. C, all control mice died by the 24th week. At the 40th week, about 40% of mice in the 30 mg/kg YC-1 group and 90% of mice in the 100 mg/kg YC-1 group were alive. D, all control mice had metastasis at the 19th week, but neither YC-1 treatment group had metastasis at that time. At the 36th week, about 70% of mice in the 30 mg/kg YC-1 group had metastasis, but metastasis was observed in only 10% of mice in the 100 mg/kg YC-1 group. E, body weight was not different among groups. F, compared with control, 30 and 100 mg/kg of YC-1 inhibited both EGFR and HIF-1α expression.

apoptosis, cell cycle progression, proliferation, differentiation, migration, and other biological processes. Hence, the abnormal expression level of EGFR is associated with cancer growth, invasion, metastasis, and resistance to chemotherapy, and it serves as a poor prognostic factor of breast cancer. Hence, anti-cancer drugs that target EGFR, such as the small molecule tyrosine kinase inhibitor gefitinib, have been widely applied to treat breast cancer[12].

EGFR, a membrane receptor possessing tyrosine kinase activity, can bind with epidermal growth factor (EGF), transforming growth factor (TGF), and amphiregulin (AR). This induces formation of homodimers or heterodimers, which triggers activation of internal tyrosine kinase activity and promotes the phosphorylation of internal tyrosine residues. Signaling downstream of the activated receptor is induced by binding of SH2 and PTB domain–containing proteins, which stimulate multiple signaling pathways such as the Jak/STAT, PI3K/Akt, and MAPK pathways. These pathways

accelerate the transition from G_1 to S phase, promote cell proliferation, and inhibit cell apoptosis [13]. At present, how YC-1 inhibits the expression of EGFR remains elusive. However, we noted in the current study that YC-1 inhibited MDA-MB-468 breast cancer cell proliferation, induced apoptosis and arrested cell cycle in G_1 phase by inhibiting EGFR expression and suppressing the downstream STAT signaling pathway, rather than by alternative pathways (unpublished results). This mechanism has been validated in nasopharyngeal carcinoma. Hong et al.[14] found that YC-1 can inhibit the proliferation, infiltration, and metastasis of nasopharyngeal carcinoma by down-regulating the expression of EGFR. Our results indicated that the stimulating effect of YC-1 on apoptosis of MDA-MB-468 cells is possibly associated with caspase 8, a finding that was also reported in another study in breast cancer cells[15]. However, Huang et al.[16] revealed that YC-1 promotes apoptosis of prostate cancer cells by activating caspase 3. Thus, it is likely that YC-1 has distinct mechanisms of action in different tumor cell types. Nevertheless, the hypothesis that YC-1 induces apoptosis through the caspase pathway has been confirmed.

HIF-1 was first discovered by Semenza et al.[17] in the nuclear extracts of Hep3B liver cancer cells as a protein that specifically binds to the erythrogenin gene enhancer. HIF-1 is an oxygen-sensitive heterodimer that consists of the HIF-1α and HIF-1β/ARNT subunits [18]. In animals, low oxygen concentration results in HIF-1α accumulation in the cytoplasm. Subsequently, HIF-1α is transferred to the nucleus, binds with HIF-1β to form the HIF-1 complex, and regulates the transcription and mRNA stability of VEGF [19]. HIF-1 complex forms consistently during the emergence of solid tumors (increasing oxygen consumption) and embryonic development (insufficient oxygen supply). HIF-1, as a central regulator genetically induced by cell balance and hypoxia, regulates the transcription of a series of target genes, including VEGF, GLUT1 and GLUT3, and plays a vital role in tumor proliferation, metastasis, and development.

YC-1 impacts various targets of HIF-1 and EGFR, and the underlying mechanism indicates that YC-1 has better clinical efficacy on breast cancer with positive EGFR expression. Our results suggest that YC-1 can significantly suppress the proliferation of breast cancer cells with high expression of EGFR, prolonging the survival of tumor-bearing nude mice, and inhibiting tumor metastasis. In addition, YC-1 yields relatively little side effects. Thus, YC-1 may be a potential treatment for breast cancers with high expression of EGFR.

Acknowledgment

References

[1] Teng CM, Wu CC, Ko FN, et al. YC-1, a nitric oxide-independent activator of soluble guanylate cyclase, inhibits platelet-rich thrombosis in mice. Eur J Pharmacol, 1997,320: 161–166.

[2] Galle J, Zabel U, Hubner U, et al. Effects of the soluble guanylyl cyclase activator, YC-1, on vascular tone, cyclic GMP levels and phosphodiesterase activity. Br J Pharmacol, 1999,127: 195–203.

[3] Chun YS, Yeo EJ, Park JW. Versatile pharmacological actions of YC-1: anti-platelet to anticancer. Cancer Lett, 2004,207:1–7.

[4] Wang SW, Pan SL, Guh JH, et al. YC-1 [3-(5-hydroxymethyl-2-furyl)-1-benzyl indazole] exhibits a novel antiproliferative effect and arrests the cell cycle in G0–G1 in human hepatocellular carcinoma cells. J Pharmacol Exp Ther, 2005,312:917–925.

[5] Zhao Q, Du J, Gu H, et al. Effects of YC-1 on hypoxia-inducible factor 1–driven transcription activity, cell proliferative vitality, and apoptosis in hypoxic human pancreatic cancer cells. Pancreas, 2007,34:242–247.

[6] Chen CJ, Hsu MH, Huang LJ, et al. Anticancer mechanisms of YC-1 in human lung cancer cell line, NCI-H226. Biochem Pharmacol, 2008,75:360–368.

[7] Chung JG, Yang JS, Huang LJ, et al. Proteomic approach to studying the cytotoxicity of YC-1 on U937 leukemia cells and antileukemia activity in orthotopic model of leukemia mice. Proteomics, 2007,7:3305–3317.

[8] Huang YT, Pan SL, J Guh JH, et al. YC-1 suppresses constitutive nuclear factor-kappaB activation and induces apoptosis in human prostate cancer cells. Mol Cancer Ther, 2005,4:1628–1635.

[9] Wu SY, Pan SL, Chen TH, et al. YC-1 induces apoptosis of human renal carcinoma A498 cells in vitro and in vivo through activation of the JNK pathway. Br J Pharmacol, 2008,155:505–513.

[10] Fallahian F, Karami-Tehrani F, Salami S, et al. Cyclic GMP induced apoptosis via protein kinase G in oestrogen receptor-positive and -negative breast cancer cell lines. FEBS J, 2011,278:3360–3369.

[11] Xia HQ, He JR. Expression of Ki-67, EGFR, HER-2 and p53 protein in human breast cancer and their correlation. Chin Clin Oncol, 2011,16:139–143. [in Chinese]

[12] Fu HY, Chen JL, Ye YJ. The development of molecular target on breast cancer. China Prac Med, 2010,15:237 –238. [in Chinese]

[13] Quesnelle KM, Boehm AL, Grandis JR. STAT-mediated EGFR signaling in cancer. J Cell Biochem, 2007,102:311–319.

[14] Hong B, Lui VW, Hui EP, et al. Reverse phase protein array identifies novel anti-invasion mechanisms of YC-1. Biochem Pharmacol, 2010,79:842−852.

[15] Lee CS, Kim YJ, Kim W, et al. Guanylate cyclase activator YC-1 enhances TRAIL-induced apoptosis in human epithelial ovarian carcinoma cells via activation of apoptosis-related proteins. Basic Clin Pharmacol Toxicol, 2011,109:283−291.

[16] Huang YT, Pan SL, Guh JH, et al. YC-1 suppresses constitutive nuclear factor-kappaB activation and induces apoptosis in human proSTATe cancer cells. Mol Cancer Ther, 2005,4:1628−1635.

[17] Semenza GL, Wang GL. A nuclear factor induced by hypoxia via *de novo* protein synthesis binds to the human erythropoietin gene enhancer at a site required for transcriptional activation. Mol Cell Biol, 1992,12:5447−5454.

[18] Sparkenbaugh EM, Saini Y, Greenwood KK, et al. The role of hypoxia inducible factor-1 alpha (HIF-1 {alpha}) in acetaminophen hepatotoxicity. J Pharmacol Exp Ther, 2011, 338:492−502.

[19] Kizaka-Kondoh S, Kuchimaru T, Kadonosono T. Pathophysiological response to hypoxia—from the molecular mechanisms of malady to drug discovery: hypoxia-inducible factor-1 (HIF-1)−active cells as a target for cancer therapy. J Pharmacol Sci, 2011,115:440−445.